Available online at www.sciencedirect.com
ScienceDirect
International Journal of Machine Tools & Manufacture 47 (2007) 1497–1506
INTERNATIONAL JOURNAL OF MACHINE TOOLS & MANUFACTURE DESIGN, RESEARCH AND APPLICATION
www.elsevier.com/locate/ijmactool

An FEM investigation into the behavior of metal matrix composites: Tool–particle interaction during orthogonal cutting

A. Pramanik, L.C. Zhang*, J.A. Arsecularatne

School of Aerospace, Department of Mechanical and Mechatronic Engineering, The University of Sydney, NSW-2006, Australia

Received 5 June 2006; received in revised form 28 November 2006; accepted 12 December 2006
Available online 8 January 2007

Abstract

An analytical or experimental method is often unable to explore the behavior of a metal matrix composite (MMC) during machining due to the complex deformation and interactions among particles, tool and matrix. This paper investigates the matrix deformation and tool–particle interactions during machining using the finite element method. Based on the geometrical orientations, the interaction between tool and particle reinforcements was categorized into three scenarios: particles along, above and below the cutting path. The development of stress and strain fields in the MMC was analyzed and physical phenomena such as tool wear, particle debonding, displacements and inhomogeneous deformation of matrix material were explored. It was found that tool–particle interaction and stress/strain distributions in the particles/matrix are responsible for particle debonding, surface damage and tool wear during machining of MMC.
© 2007 Elsevier Ltd. All rights reserved.

Keywords: Metal matrix composite; Tool–particle interaction; Finite element method

1. Introduction

Metal matrix composites (MMCs), particularly aluminum-based particle/fiber-reinforced composites, have a high strength to weight ratio and therefore are increasingly used in automotive and aerospace structures. The research on discontinuous particulate/fiber-reinforced MMCs has been a focus these days because of their low manufacturing cost, ease of production, and macroscopically isotropic mechanical properties [1–3].

In a monolithic metal, matrix metal is the load transferor as well as a load carrier. However, the nature of load bearing by a composite depends on the type of its components. For a continuous fiber reinforced MMC, the fibers are load carriers and the metal matrix is the transferor. For a discontinuous particle/fiber-reinforced MMC, both the matrix and reinforcement are the load carriers and load transferors [2]. In a study of local deformation behavior of MMCs by tensile loading experiments, Unterweger et al. [4] noted (through observation by scanning electron microscope) inhomogeneous deformation of matrix material in a banded pattern which was controlled by particle size and arrangements.

The machining mechanism of particle-reinforced MMCs is expected to be different from others. Numerous reports can be found in the literature describing the experimental studies related to the machining of MMCs, but analytical [5,6] and numerical [7–10] investigations are few. Notably, Pramanik et al. [5] and Kishawy et al. [6] developed force prediction models based on material removal mechanisms and energy for material deformation and particle debonding/fracture, respectively. Monaghan and Brazil [7] modeled the machining (by FORGE2 code) of A356 aluminum alloy and then submodeled (by ANSYS software) different regions of the chip and the machined surface of MMC. They studied non-uniform matrix flow, tool wear, failure of particle–matrix interface, change of loading (in different submodels) and the generated residual stress in MMC surface due to applying the pressure and temperature obtained from aluminum alloy machining simulation. This is not realistic as response of cutting MMC is completely different from that of a monolithic alloy though the work was a commendable attempt to find the effects of machining

*Corresponding author. Tel.: +61 2 93512835; fax: +61 2 93517060.
E-mail address: zhang@aeromech.usyd.edu.au (L.C. Zhang).

0890-6955/$ - see front matter © 2007 Elsevier Ltd. All rights reserved.
doi:10.1016/j.ijmachtools.2006.12.004

on the generated surface and tool indirectly. Moreover, their study was unable to investigate some of the important phenomena such as surface damage and tool–particle interaction during machining of MMC. In El-Gallab et al's [8] finite element study, nearly the same modeling procedure as in Ref. [7] was followed except that forces and temperatures applied on the MMC surface were obtained from MMC machining. Their objective was to select the cutting parameters from a set of experimental results that would result in minimum subsurface damage and the least tool wear. The ratio of the hydrostatic stress beneath the machined surface to the shear flow strength (obtained from finite element simulation) was the basis to detect surface quality. It was assumed that higher the above ratio, less likely was the subsurface damage. Although incorporation of reinforcements in their model was stated, the effects of reinforcements in the obtained results are not clear. Ramesh et al. [9] carried out a transient dynamic finite-element analysis to investigate the mechanics of diamond turning of an Al6061/SiC MMC. They studied the possible encounters of the tool that included tool facing SiC/matrix and tool ploughing SiC/matrix, and considered frictionless point contact between the tool and workpiece. They presented the range of forces and stresses that could be generated during micro-machining of MMC. However, the structure of MMC considered was not as in practice, e.g., when the tool facing SiC, the layer of material corresponding to cut thickness was assumed to be SiC and the remainder aluminum. When the tool facing aluminum, the layer of material corresponding to cut thickness was assumed to be aluminum and the remainder SiC. Thus their model was not able to account for tool interacting with SiC and matrix simultaneously. Zhu and Kishawy [10] developed a plane-strain thermo-elastic–plastic finite element model to simulate orthogonal machining of Al6061/Al_2O_3 composite using a tungsten carbide tool. They reported the average values of effective and shear stresses in the matrix and on particles at different locations in the chip and primary/secondary deformation zones, and temperature distribution in the matrix macroscopically. The normal and shear stresses at tool–chip interface were used to explain crater wear. Although rectangular reinforcement particles seem to be incorporated in their FE model, it was not able to describe physical phenomena such as particle debonding, tool–particle interaction and their effects on surface integrity.

Another group of study was the combination of analytical solution with experimentation that involved scratching and wear of particle reinforced MMCs. Zhang et al. [11] studied particles' effects on friction and wear of 6061 aluminum alloy reinforced with silicon carbide and alumina particles by means of Vickers microhardness measurements and scratch tests. They explored the effects of heat treatment for three different conditions: under-aged, over-aged and T6. It was concluded that T6 heat-treated composites have the highest hardness and friction coefficient while the peak-aged composites exhibit the best wear resistance. The wear rate of fine particle-reinforced composites was mainly affected by hardness but that for large particle-reinforced composites was influenced by both the hardness and fracture of the particles. In another study, Yan and Zhang [12] investigated the cutting mechanism and the relationship between specific energy and depth of cut by single point scratch test on alumina and silicon carbide reinforced aluminum alloy (6061). They proposed a simple model to interpret the apparent size effect. The effect of reinforcement on the specific energy was accounted by using the ratio of volume fraction to particle radius. The effects of the ceramic particles on the transition load (from mild to severe wear) and wear for varying normal pressure were studied by Zhang et al. [13]. They identified three wear mechanisms that included abrasion (in the running-in period), oxidation (during steady wear at low load levels) and adhesion (at high loads). A higher particle volume fraction was found to raise the transition load but increased the wear rate in the abrasion and adhesion regimes. Increase of particle size was more effective than increase of volume fraction to prolong the transition from mild wear to adhesive wear. They also proposed a criterion based on dislocation and delamination theories for determining the critical transition load and developed quantitative models for steady sliding [14] and adhesive wear [15] in a wear system of a steel disc sliding against MMC pins. The models predicted that the wear is proportional to the applied load and depends on the particle volume fraction of the composite and the relative hardness of the rubbing pair. The criterion and the wear models were validated by experiments.

It is clear that presence of reinforcement makes MMCs different from monolithic materials and induces superior physical properties to MMC. On the other hand, these reinforcement particles are responsible for very high tool wear and inferior surface finish when machining MMCs. Thus tool–particle interactions and their effects are important issues in machining of MMCs [5,6,10]. However, a detailed investigation of tool–particle interactions and their consequences is still lacking but is needed for a better understanding of process outcomes such as tool wear, surface finish, residual stresses, cutting forces, etc.

The purpose of this paper is to investigate tool–particle interaction, residual stresses, etc. during machining of MMCs with the aid of the finite element method. The development of stress/strain fields is explored for various tool–particle orientations and analyzed for possible particle fracture, debonding, etc., to provide an insight for understanding the mechanism of MMC machining.

2. Modeling

2.1. Boundary conditions

A two-dimensional finite element model was constructed using explicit finite element software package ANSYS/LS-DYNA, version 10. Lagrangian formulation was used for

material continuum to develop the plane-stress model. The geometry of machining is shown in Fig. 1. In accordance with practice, the tool cutting edge was assumed to have a 6 μm edge radius. The reinforcement particles were introduced around the cutting line and restricted to a small area to keep the model size manageable. In order to facilitate the study of particle interaction at different locations of the tool rake face and rounded cutting edge, rows of reinforcements were inclined to the cutting direction. The particles (18 μm diameter) were 20% by volume in this region and were assumed to be perfectly bonded with the matrix. Similar to the work reported in [16,17], the interface nodes of the matrix and reinforcements were tied together, therefore the initial displacements at the interface are equal for both the matrix and reinforcements. Since the interface is very hard and brittle and hence similar to the particles [10], the interface was considered as an extension of the particle. The cutting tool was treated as a rigid body and moved horizontally into the workpiece at a predetermined speed with the cut thickness = 0.2 mm. The tool movement was constrained in all other directions. The cutting speed was kept reasonably low (50 m/min) and it was assumed, for simplicity, that the cutting temperature has negligible influence on material properties. It was reported that, at cutting speed around 50 m/min, depth of cut 1 mm and feed 0.1 mm/rev, the temperature is approximately 105 °C for machining MMC with 30% SiC (vol) reinforcement [18]. At this temperature the change of material properties was negligible [19]. In addition, a correlation between strength of MMC and cutting speed was established in [5] for depth of cut 1 mm and feed = 0.2 mm/rev. From that relation it was found that due to cutting speed of 50 m/min the strength of MMC was reduced only by 0.25%. This reduction of strength can be neglected to avoid complexity. The workpiece was fully fixed on its bottom surface to eliminate rigid body motion.

2.2. Material model

The MMC work material was a 6061 aluminum alloy reinforced with silicon carbide particles. A temperature-independent plastic kinematic material model (from ANSYS/LS-DYNA [20]) and associative flow rule were used for the matrix. Strain rate was accounted for using the Cowper-Symonds model which scaled the yield stress by a strain rate dependent factor. According to ANSYS/LS-DYNA manual [20] the equation to calculate yield stress in the plastic kinematic material model is given below

$$\sigma_y = \left[1 + \left(\frac{\dot{\varepsilon}}{C}\right)^{1/P}\right](\sigma_0 + \beta E_p \varepsilon_p^{eff}), \tag{1}$$

where

$$E_p = \frac{E_{tan} E}{E - E_{tan}}, \tag{2}$$

Here σ_y, is the yield stress, σ_0, the initial yield stress, $\dot{\varepsilon}$, the strain rate, C and P are the Cowper-Symonds strain rate parameters, ε_p^{eff}, the effective plastic strain, β, the hardening parameter ($\beta = 0$ for kinematic hardening and 1 for isotropic hardening [20]) and E_p, the plastic hardening modulus, E_{tan}, the tangent modulus, E, the modulus of elasticity. The material properties of the matrix were based on the commonly accepted values $\sigma_0 = 125$ MPa, $E = 71$ GPa, $E_{tan} = 1.48$ GPa from [21,22]. Values of Cowper-Symonds strain rate parameters ($C = 6500$, $P = 4$) for alluminum alloy were taken form ANSYS/LS-DYNA manual [20]. In this study kinematic hardening was considered as a first assumption because of comparatively

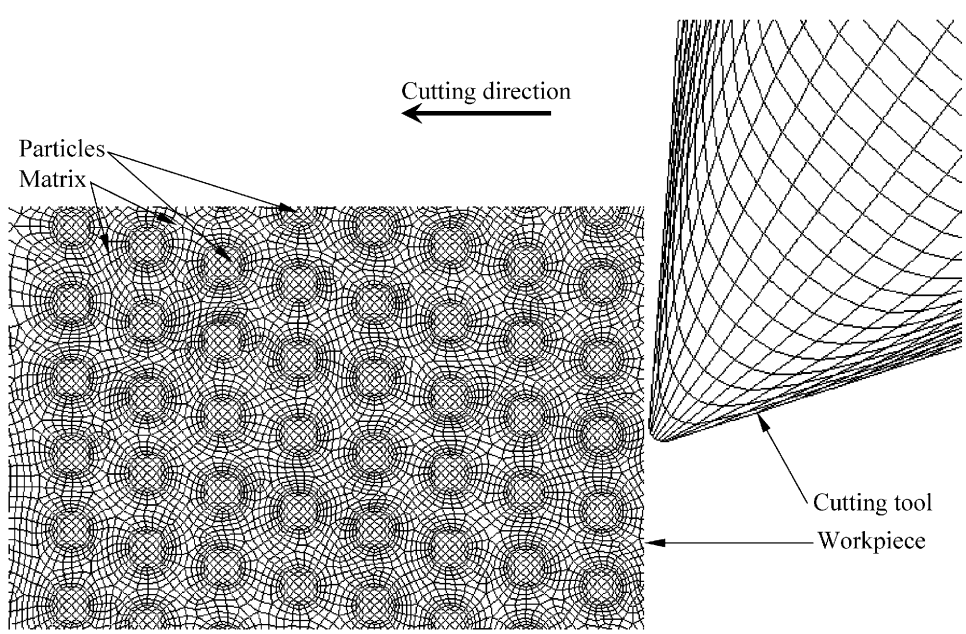

Fig. 1. Workpiece and tool for MMC machining simulation.

low plastic hardening modulus (1.51 GPa) of matrix material and to investigate the strain rate effect.

A chip separation criterion available with ANSYS/LS-DYNA for this material model was used in the simulation. According to this criterion, chip separation occurs when the strain value of the leading node is greater than or equal to a limiting value. Based on the work for aluminum alloys reported in [13], the limiting strain was taken as 1. When an element of matrix material reached the limiting strain value, the corresponding element would be deleted. Additionally, SiC particles were treated as an isotropic perfectly elastic material following the generalized Hook's law. For simplicity, particle fracture was not considered in the present model and debonding of particles was assumed to be due to failure of the matrix material around the particles. The material properties of the particles were based on the commonly accepted values: modulus of elasticity = 400 GPa and Poisson's ratio = 0.17.

2.3. Contacts during machining

Along with the general contact family in ANSYS/LS-DYNA, the automatic contact options are the most commonly used contact algorithms for its versatility. Hence, 2D automatic contact was chosen for this simulation. In order to consider the effect of friction along the tool–chip interface, Coulomb friction model was employed. This is defined as

$$\tau_{\lim} = \mu P + b, \tag{3}$$

$$|\tau| \leqslant \tau_{\lim}, \tag{4}$$

where $\tau_{\lim}$, is the limiting shear stress, τ, the equivalent shear stress, P, the contact pressure, μ, the friction coefficient and b, the cohesion sliding resistance (sliding resistance with zero normal pressure). According to ANSYS/LS-DYNA manual [20], two contacting surfaces can carry shear stresses up to a certain magnitude across their interface before they start sliding relative to each other (sticking state). When $\tau > \tau_{\lim}$, the two surfaces will slide relative to each other (sliding state). For machining conditions b was assumed to be zero. The limiting shear stress $\tau_{\lim} = 202$ MPa and coefficient of friction, $\mu = 0.62$ were based on the study reported in [5].

3. Results and discussion

When a cutting tool removes a layer from the MMC workpiece, the uncut layer is first elastically deformed followed by plastic deformation and chip formation near the cutting edge of the tool. An element of material to be removed is initially under no stress when it is well ahead of the tool. As the tool approaches, the material enters a region of high strain rate where plastic deformation occurs, and becomes part of the chip. During the process of chip formation, some reinforcements in the cutting region will go into the chip, some will be debonded/fractured and the rest will be on the machined surface. In the present investigation, the interaction between the tool and reinforcements is categorized into three scenarios: particles along the cutting path, particles above the cutting path and particles below the cutting path (Fig. 2). All these cases, with the advancement of cutting tool during machining, are discussed in detail in the following sections.

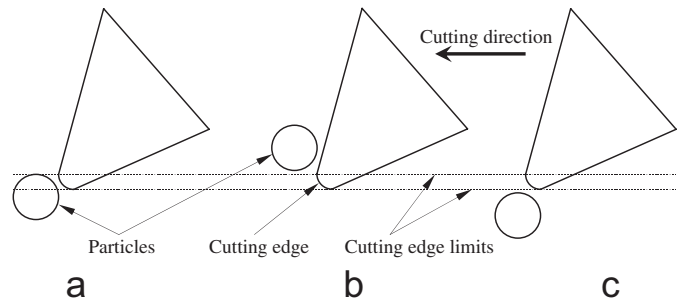

Fig. 2. Particle locations with respect to the cutting path: particles (a) along, (b) above, and (c) below the cutting path.

3.1. Evolution of stress field

The evolution of stress fields in particles, interfaces and the surrounding matrix during machining of MMC are now considered.

3.1.1. Scenario 1: particles along the cutting path

The orientation between tool and particle is categorized under this case if any part of a particle falls in between upper and lower limits of cutting edge as shown in Fig. 2(a). The evolution of stress fields during machining is demonstrated in Figs. 3(a)–(d) for a particle located in the lower part of the cutting edge, i.e., the center of particle is below the center of the cutting edge. Initially the compressive and tensile stresses are perpendicular and parallel, respectively, to the cutting edge in the matrix and particle in front of the cutting edge. This type of stress distribution may initiate fracture in the particle and debonding at the interface. With the advancement of the tool, the matrix between the upper part of the particle and tool becomes highly compressive while lower right interface of the particle becomes highly tensile (Fig. 3a). This indicates that an anticlockwise moment is acting on the particle, thus debonding of the particle may be expected with further advancement of the tool. When tool–particle interaction occurs, significant tensile and compressive stresses that are perpendicular to each other are found in the left part of the particle (Fig. 3b). However, the right part of the particle is only under compressive stress. Such stress distribution may initiate particle fracture if the stresses are high enough. With further advancement of the tool, the particle debonds and ploughs through the matrix making a cavity, then slides on the cutting edge and flank face (Fig. 3c), and becomes almost stress-free (Fig. 3d).

The stress field evolution for a particle located at the upper part of the cutting edge is demonstrated in Figs. 3(c)

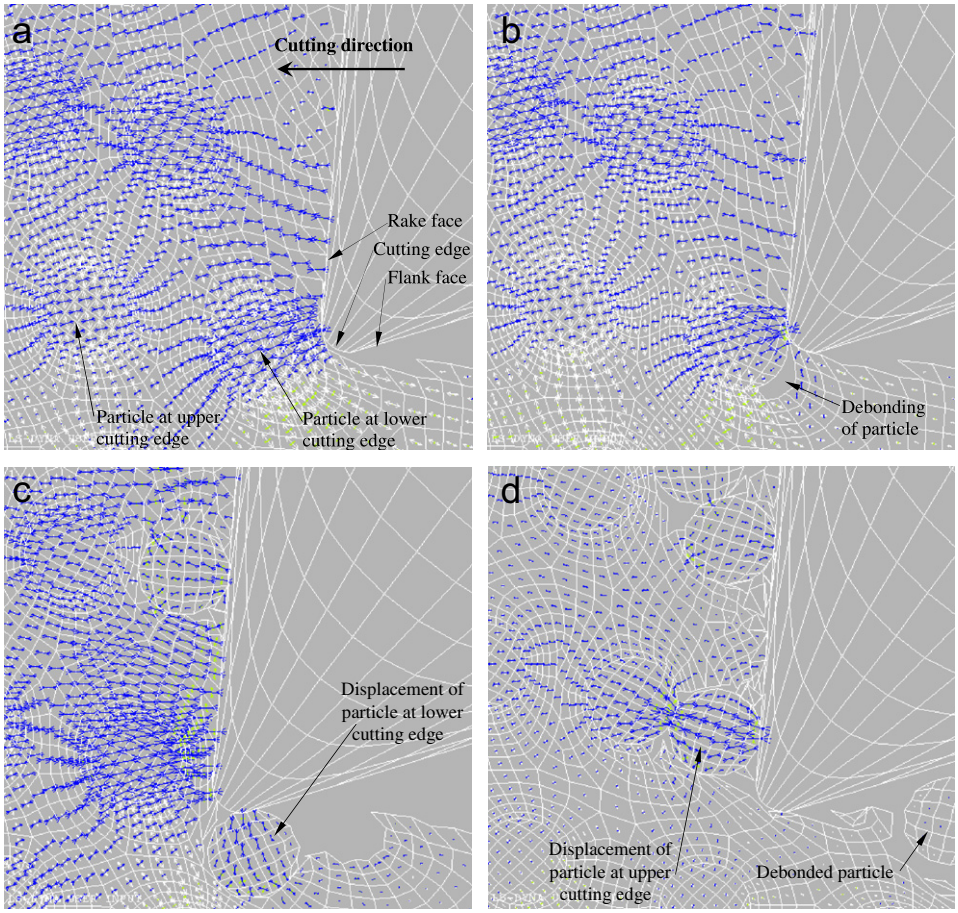

Fig. 3. Evolution of stress fields for particle along the cutting path during machining of MMC. Compressive and tensile stresses are represented by blue/black >–< and white <—> symbols, respectively. Their lengths represent comparative magnitudes.

and (d). Due to the plastic flow of the matrix this particle has moved slightly upwards. Initially the matrix in between the particle and tool is under high compressive stress acting parallel to cutting direction with no tensile stress (Fig. 3c). On the other hand, a part of the particle and interface are under compressive stress along the cutting direction and under tensile stress perpendicular to the cutting direction. This type of stress distributions can lead to particle debonding and/or fracture. After interacting with the tool's rake face, the particle partially debonds and moves up with the chip. With further advancement of the tool (Fig. 3d) it then interacts with a nearby particle and consequently both particles are under high compressive stress applying perpendicular to the rake face. This high compressive stress may cause fracture of the particle as well as wear on the tool rake face. Interaction of this particle with the second particle generates a similar stress distribution in the latter which can initiate its fracture and debonding. Additionally, stress in the surrounding matrix has reduced, possibly due to debonding of the particles.

3.1.2. Scenario 2: particles above the cutting path

A typical orientation of particle for this case is presented in Fig. 2(b). The evolution of stress field in the MMC is presented in Figs. 4(a) and (b). Initially high compressive stress field perpendicular to tool rake face through the particle and in the matrix in between particle and rake face is noted. At the same time, part of the particle and interface are under compressive (perpendicular to rake) and tensile (parallel to rake) stresses as shown in Fig. 4(a). As stated before, this type of stress distribution may initiate particle fracture and interface debonding. As the tool proceeds, it interacts and partially debonds the particle. The contact region with the rake face is under high compressive stress, hence fracture of the particle can be expected. At this stage the matrix in between this particle and next one is also under very high compressive stress. With further advancement of the tool, the first particle interacts with the next particle and moves up along the rake face under high compressive stress (Fig. 4b).

3.1.3. Scenario 3: particles below the cutting path

Fig. 2(c) represents this type of tool–particle orientation. The stress distribution in the particle and matrix below the cutting edge has a direct influence on the residual stress of the machined surface. Figs. 5(a)–(c) shows the evolution of stress field for a particle below the cutting edge. As the tool approaches the particle, the matrix in between the cutting edge and particle is under compressive stress acting in a radial direction to the cutting edge. However, the particle

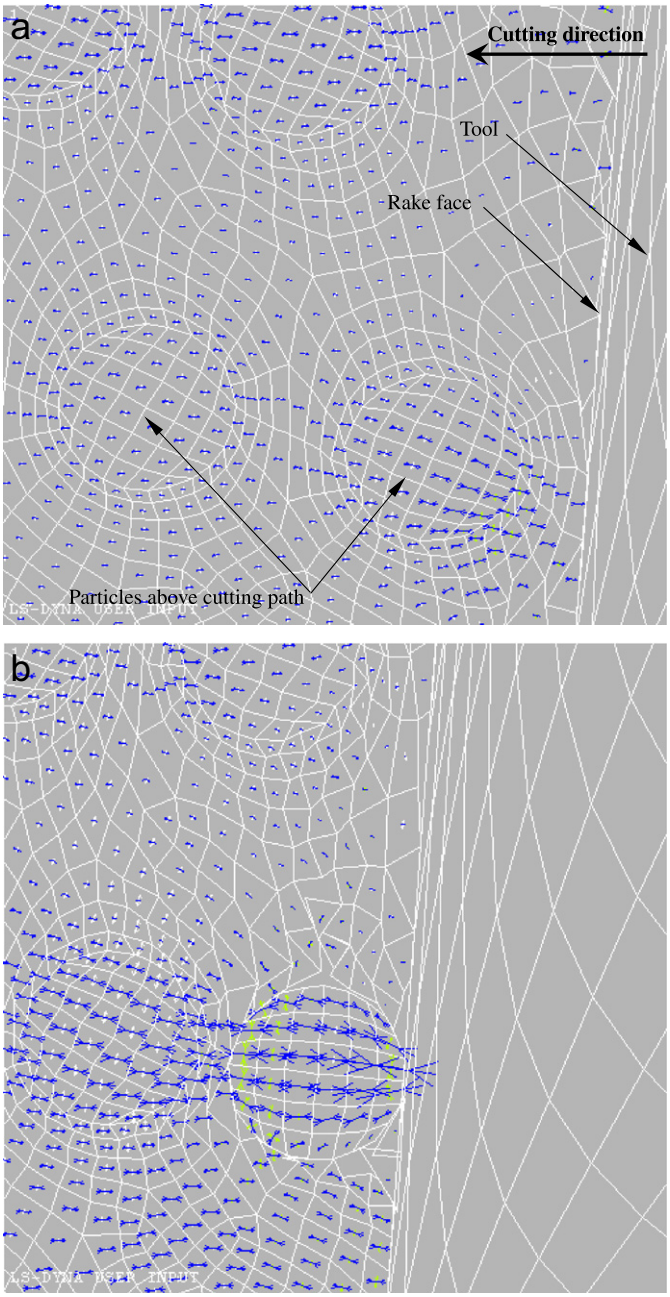

Fig. 4. Evolution of stress fields for particle above the cutting path during machining of MMC. Compressive and tensile stresses are represented by blue/black >–< and white <—> symbols, respectively. Their lengths represent comparative magnitudes.

and particle–matrix interface are under compressive and tensile stresses which are acting in a radial direction to the cutting edge and parallel to the cutting edge, respectively (Fig. 5a). While the tool is passing over the particle, the direction of compressive stress remains radial to the cutting edge. On the other hand, the direction of tensile stresses in the particle becomes parallel to machined surface (Fig. 5b). At the same time, the magnitudes of both stresses have decreased. It is also noted that the newly generated surface is under compressive residual stress which is parallel to the machined surface (Fig. 5c). Similar observations were also reported in an experimental study by Quan et al. [24], who machined SiC particulate reinforced MMC.

3.2. Development of the plastic zone

Figs. 6(a)–(f) depict the contours of the von Mises plastic strain in the MMC material at different stages of machining. Plastic deformation is observed as the workpiece material enters into the primary deformation zone. The distribution of plastic strain is in layered pattern with a highly strained zone at the tool–chip interface. Plastic strain has clearly increased as the material moves into the chip. However, the particles are well discerned because no plasticity exists in purely elastic particles. Moreover, the deformation patterns are different compared to those of monolithic metal during machining in that the presence of discrete particles causes banded structure and dramatically fragments the plastic field.

3.2.1. Particles along the cutting path

Initially, for a particle at lower part of the cutting edge, the matrix in between particle and tool, and that at upper part of particle are highly strained (Fig. 6a). With the progression of cutting, tool interacts with the particle at cutting edge and the particle is debonded. It then slides and indents (Figs. 6b and c) into the new workpiece surface causing high plastic strain in the surrounding matrix. As the tool moves further, the particle is released from matrix leaving a ploughed hole in the surface with high residual strain (Fig. 6d).

A particle located at the upper part of cutting edge moves up slightly with the advancement of tool (Fig. 6c). In this case, the strain in the matrix in between the particle and tool is not as high as the strain for a particle at lower part of cutting edge discussed earlier. The interaction between the particle and tool is observed in this case with further progression of tool (Fig. 6d). Then the particle partially debonds and slides along the rake face with the chip (Fig. 6e).

3.2.2. Particles above the cutting path

At first, particles move in the cutting direction with the surrounding matrix due to the movement of the tool. As the rake face of the tool approaches, particle interface becomes highly strained (Fig. 6b). Due to the ability of the matrix to deform plastically and particle's inability, the matrix material experiences very high plastic strain. With further advancement of the tool, particles debond partially, interact with the tool and nearby particles, and move with the chip along the rake face (Figs. 6c–e). At the secondary deformation zone (tool–chip interface), matrix experiences severe deformation, hence interfaces of most particles in the chip are highly strained. Additionally, most of the particles debond completely while passing through the secondary deformation zone (Fig. 6f).

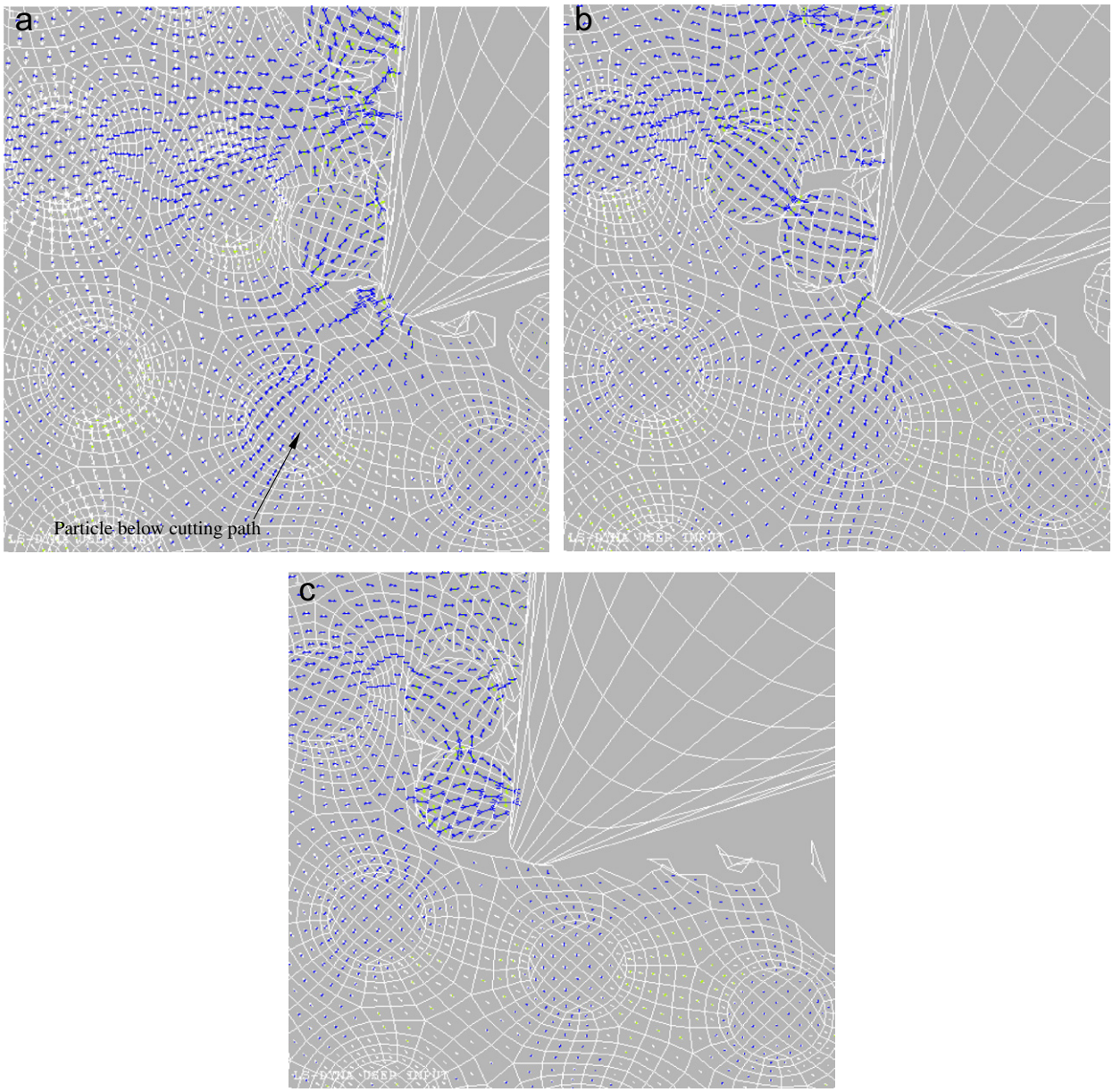

Fig. 5. Evolution of stress fields for a particle below the cutting path during machining of MMC. Compressive and tensile stresses are represented by blue/black >–< and white <—> symbols, respectively. Their lengths represent comparative magnitudes.

3.2.3. Particles below the cutting path

The interfaces of particles in the workpiece far below the cutting edge do not experience any plasticity due to machining. But those situated immediately below the cutting edge are subjected to plastic deformation when the tool passes over them (Fig. 6e). The banded pattern of the strain field is fragmented in the interface of particles just below the tool cutting edge. With further advancement of the tool, most of the interface of the particle is plastically deformed (Fig. 6e). Additionally, the matrix at the matrix–tool cutting edge interface is plastically strained. The particles immediately below the cutting edge seem to act like indenters due to their interaction with the tool. In these regions the matrix can be seen to plastically deformed to a greater depth (Fig. 6f).

3.3. Comparison of experimental and FE simulation observations

3.3.1. Particles along the cutting path

From the finite element simulations it is observed that particles in the lower part of the cutting edge initially interact with cutting edge and are then debonded leaving a cavity on the machined surface. They also take part in ploughing of the newly generated work surface. The particles in the upper part of the cutting edge slide over the rake face. It is expected that, with the increase of cutting speed, the impact between tool and particles will increase.

Repeated interaction, which generates high stress concentration, and sliding of particles on lower part of cutting

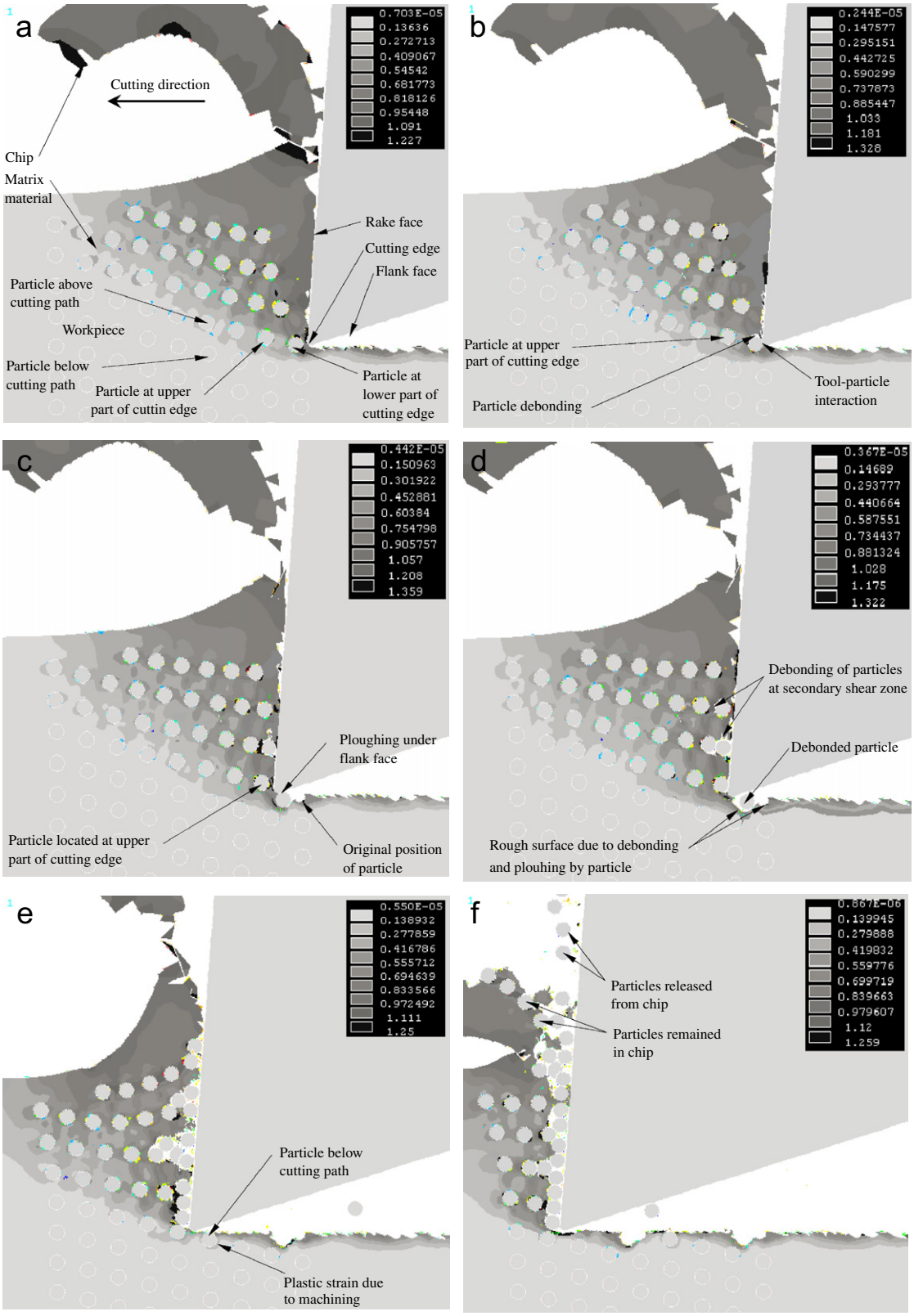

Fig. 6. Distribution of von Mises strain during machining of MMC.

edge and tool flank may create groves, cracks and pull out of tool material particles from cutting edge and flank face during machining of MMC. Several researchers [25–27] reported the grooves and chipping (due to repeated impact between tool edge and particles) on the cutting edge and flank face after machining MMCs. The damage of the tool cutting edge/flank was attributed to abrasion [23,25,28,29] and pull out of tool material grains from cutting edge and

flank face of the tool [27]. It was also reported that flank wear increases with the increase of speed [30,31] and at high speeds, chipping of cutting edge becomes prominent [31]. Under these conditions, impact between particle and tool increases which induces easier fracture causing chipping at the cutting edge.

After interacting with the cutting edge and flank face, particles on the lower part of the cutting edge are debonded and pulled out leaving cavities on the machined surface. Zhang et al. [11] and, Yan and Zhang [12] who studied MMCs by scratching tests observed pull out of reinforcement particles and cavities on the scratched surface. Similar observations were also reported in an experimental study by El-Gallab et al. [32] who machined SiC particulate reinforced MMC.

3.3.2. Particles above the cutting path

The beginning of flow of particles in the chip root region was observed at the start of MMC machining and with further advancement of the tool, the inter particle distance as well as distance between particle and tool decrease. Cracking seems to occur from partial debonding of particles from the matrix near the secondary shear zone in front of the cutting tool (Figs. 6c–e). The interfaces of reinforcement particles fail as they go through the secondary shear zone. Thus, the partially debonded particles interact with nearby particles as well as with tool which results in further debonding and gathering of particles on the rake face (Figs. 6e and f). These particles slide continuously over the rake face and go in to the chip (Fig. 6f). During sliding they may scratch the tool rake face leading to abrasive wear. This is different to the flank where impact and discontinuous sliding of particles were noted. Hence smoother wear at rake is expected. After sliding few hundred microns along rake face, some particles are dislodged from chips while others remain in chips (Fig. 6f).

It is of interest to note that the above-mentioned phenomena were noted in experimental investigation by Hung et al. [33] who used a quick stop device. They reported cracks due to debonding of particles in front of tool. In the chip root region, reinforced particles were observed to align along the shear plane. El-Gallab and Sklad [32] studied chips obtained from machining MMC and observed the flow lines of particles and debonded particles in the chips.

Almost all researchers noted comparatively high tool wear during machining of MMC with any tool. For diamond tools it is reported that wear at rake face is also abrasive but smoother than that at flank face [25,26,34]. The rake face wear can be attributed to frequent interactions between the rake face and hard particles, and the continuous sliding of these particles along the rake face (Figs. 6e and f).

3.3.3. Particles below the cutting path

Direct tool–particle interactions do not happen when particles are well below the cutting edge but the tool movement causes a significant change in stress in the particles and stress/strain in the surrounding matrix. The degree of plastic deformation of the newly generated surface depends on the particle orientations. These cause inhomogeneous deformation and flow of matrix in the MMC (Fig. 6f). Thus localized hardening of MMC surface can be expected after machining. In this scenario the effect of cutting tool edge on the workpiece surface may resemble the indentation of an MMC. Pramanik et al. [17] studied micro-indentation of MMC and noted inhomogeneous deformation of matrix material due to presence of particles. Particle orientations were found to play an important role on the degree of plastic deformation of matrix material. Matrix at particle–matrix interface and that between particle and tool were shown to be highly strained. These phenomena were also observed by other researchers, e.g., Monaghan and Brazil [7] who numerically studied micromechanics associated with the machining of particle reinforced MMCs noted inhomogeneous matrix flow in the machined surface which was controlled by reinforced particles.

4. Conclusions

A finite element model is used for orthogonal machining simulation of SiC particle reinforced aluminum matrix based MMCs. A complex issue, i.e. tool–particle interaction during machining, was analyzed using the stress/strain fields developed. Good qualitative agreement was noted between obtained results from this investigation and the experimental results available in the literature. The following conclusions can be drawn from the present analysis:

(a) The magnitude and distribution of stresses/strains in the MMC material and interaction of particles with the cutting tool are the main reasons for particle fracture and debonding during machining of MMC.
(b) The indentation of particles (located immediately below the cutting edge) due to their interaction with the tool causes localized hardening of machined MMC surface. In these regions, the matrix can be seen to plastically deform to a greater depth.
(c) Newly generated surfaces are under compressive residual stress. Moreover, these surfaces are damaged due to cavities left by the pull-out of particles. These cavities are formed when particles located at the lower part of the cutting edge interact with the cutting tool.
(d) High tool wear during machining of MMCs is due to sliding of debonded particles over cutting edge and tool faces that will scratch these contact surfaces.

Acknowledgements

The authors wish to thank the Australian Research Council for financial assistance. A.P. has been supported by IPRS and IPA.

References

[1] Z. Wang, T. Chen, D.J. Lloyd, Stress distribution in particulate-reinforced metal-matrix composites subjected to external load, Metallurgical Transactions 24A (1993) 197–207.

[2] D. Huda, M.A. El Baradie, M.S.J. Hashmi, Analytical study for the stress analysis of metal matix composites, Journal of Materials Processing Technology 45 (1994) 429–434.

[3] N. Shi, R.J. Arsenault, Analytical evaluation of the thermal residual stresses in Si/Al composites, JSME International Journal, Series 1 34 (2) (1991) 143–155.

[4] K. Unterweger, O. Kolednik, The local deformation behaviour of MMCs—an experimental study, Material Research and Advanced Techniques 96 (9) (2005) 1063–1068.

[5] A. Pramanik, L.C. Zhang, J.A. Arsecularatne, Prediction of cutting forces in machining of metal matrix composites, International Journal of Machine Tools and Manufacturing 46 (2006) 1795–1803.

[6] H.A. Kishawy, S. Kannan, M. Balazinski, An energy based analytical force model for orthogonal cutting of metal matrix composites, Annals of the CIRP 53 (1) (2004) 91–94.

[7] J. Monaghan, D. Brazil, Modelling the flow processes of a particle reinforced metal matrix composite during machining, Composites 29A (1998) 87–99.

[8] M.S. El-Gallab, M.P. Sklad, Machining of aluminum/silicon carbide particulate metal matrix composites. Part IV: residual stresses in the machined workpiece, Journal of Material Processing Technology 152 (2004) 23–34.

[9] M.V. Ramesh, K.C. Chan, W.B. Lee, C.F. Cheung, Finite-element analysis of diamond turning of aluminium matrix composites, Composites Science and Technology 61 (2001) 1449–1456.

[10] Y. Zhu, H.A. Kishawy, Influence of alumina particles on the mechanics of machining metal matrix composites, International Journal of Machine Tools and Manufacturing 45 (2005) 389–398.

[11] Z.F. Zhang, L.C. Zhang, Y.W. Mai, Particle effects on friction and wear of aluminium matrix composites, Journal of Materials Science 30 (23) (1995) 5999–6004.

[12] C. Yan, L.C. Zhang, Single-point scratching of 6061 Al alloy reinforced by different ceramic particles, Applied Composite Materials 1 (1995) 431–447.

[13] Z.F. Zhang, L.C. Zhang, Y.W. Mai, Wear of ceramic particle-reinforced metal-matrix composites, Part I: wear mechanisms, Journal of Materials Science 30 (8) (1995) 1961–1966.

[14] Z.F. Zhang, L.C. Zhang, Y.-W. Mai, Modeling steady wear of steel/Al_2O_3-Al particle reinforced composite system, Wear 211 (2) (1997) 147–150.

[15] Z.F. Zhang, L.C. Zhang, Y.W. Mai, Wear of ceramic particle-reinforced metal-matrix composites, Part II: a model of adhesive wear, Journal of Materials Science 30 (8) (1995) 1967–1971.

[16] J. Monaghan, D. Brazil, Modeling the sub-surface damage associated with the machining of particle reinforced MMC, Computational Materials Science 9 (1997) 99–107.

[17] A. Pramanik, L.C. Zhang, J.A. Arsecularatne, Micro-indentation of metal matrix composites—an FEM analysis, in: The Eighth Asia-Pacific Symposium on Engineering Plasticity and its Applications (AEPA-2006), September 25–29, 2006, Nagoya, Japan.

[18] R.R. Reddy, A.A. Sriramakrishna, Analysis of orthogonal cutting of aluminium-based composites, Defence Science Journal 52 (4) (2002) 375–383.

[19] T.W. Clyne, P.J. Withers, in: E.A. Davis, I.M. Ward (Eds.), An Introduction to Metal Matrix Composites, Cambridge University Press, Cambridge, 1993, p. 266.

[20] ANSYS/LS-DYNA Reference Manual, Release 10, Livermore Software Technology Corporation, Livermore, CA. www.lstc.com.

[21] G. Meijer, F. Ellyin, Z. Xia, Aspects of residual thermal stress/strain in particle reinforced metal matrix composites, Composites: Part B 31 (2000) 29–37.

[22] S.G. Long, Y.C. Zhou, Thermal fatigue of particle reinforced metal–matrix composite induced by laser heating and mechanical load, Composites Science and Technology 65 (2005) 1391–1400.

[23] S.P.F.C. Jaspers, J.H. Dautzenberg, Material behaviour in metal cutting: strains, strain rates and temperatures in chip formation, Journal of Material Processing Technology 121 (2002) 123–135.

[24] Q. Yanming, Y. Bangyan, The effect of machining on the surface properties of SiC/Al composites, Journal of Materials Processing Technology 138 (1–3) (2003) 464–467.

[25] M. El-Gallab, M. Sklad, Machining of Al/SiC particulate metal matrix composites, Part I: tool performance, Journal of Material Processing Technology 83 (1998) 151–158.

[26] X. Ding, W.Y.H. Liew, X.D. Liu, Evaluation of machining performance of MMC with PCBN and PCD tools, Wear 259 (2005) 1225–1234.

[27] A.R. Chambers, The machinability of light alloy MMCs, Composites: Part A 27A (1996) 143–147.

[28] C.B. Lin, Y.W. Hung, W.-C. Liu, S.-W. Kang, Machining and fluidity of 356Al/$SiC_{(p)}$ composites, Journal of Material Processing Technology 110 (2001) 152–159.

[29] J.P. Davim, Diamond tool performance in machining metal-matrix composites, Journal of Material Processing Technology 128 (2002) 100–105.

[30] E. Kılıçkap, O. Çakır, M. Aksoy, A. İnan, Study of tool wear and surface roughness in machining of homogenised SiC-p reinforced aluminium metal matrix composite, Journal of Materials Processing Technology 164–165 (2005) 862–867.

[31] I. Ciftci, M. Turker, U. Seker, Evaluation of tool wear when machining SiC_p-reinforced Al-2014 alloy matrix composites, Materials and Design 25 (2004) 251–255.

[32] M. El-Gallab, M. Sklad, Machining of Al/SiC particulate metal matrix composites, Part II: work surface integrity, Journal of Material Processing Technology 83 (1998) 277–285.

[33] N.P. Hung, N.L. Loh, V.C. Venkatesh, Machining of metal matrix composites, in: S. Jahanmir, M. Ramulu, P. Koshy (Eds.), Machining of Ceramics and Composites, Marcel Dekker Inc., New York, 1999.

[34] P.J. Heath, Developments in applications of PCD tooling, Journal of Material Processing Technology 116 (2001) 31–38.